Journal of Applied Polymer Science

Eco-Friendly, Acrylic Resin-Modified Potassium Silicate as Water-Based Vehicle for Anticorrosive Zinc-Rich Primers

Iman Mirzaie Goodarzi,[1] Mansour Farzam,[1] Mohammad Reza Shishesaz,[1] Davood Zaarei[2]
[1]Abadan Faculty of Petroleum Engineering, Petroleum University of Technology, Abadan, Iran
[2]Technical Faculty, South Tehran Branch, Islamic Azad University, Tehran, Iran
Correspondence to: M. Farzam (E-mail: mansour.farzam@gmail.com)

ABSTRACT: Potassium silicate binder of zinc-rich coating was modified by adding water-based acrylic resin. Several series of coatings containing 5, 10, and 15 wt % of acrylic and acrylic/styrene binders were added to potassium silicate. The coatings were applied on steel and the corrosion resistance of coatings was evaluated by conventional methods such as electrochemical impedance spectroscopy, corrosion potential, salt spray, and scanning electron microscopy. The results indicated that the modification of silicate binder with acrylic and acrylic/styrene led to shortening the curing time, improved corrosion protection, better dispersion of zinc particles, and enhanced salt spray resistance of resultant coatings. © 2014 Wiley Periodicals, Inc. J. Appl. Polym. Sci. **2014**, *131*, 40370.

KEYWORDS: coatings; electrochemistry; zinc-rich; resins

Received 27 October 2013; accepted 30 December 2013
DOI: 10.1002/app.40370

INTRODUCTION

Using zinc-rich coatings is a very efficient method for protecting steel structures against corrosion.[1–7] The waterborne inorganic zinc-rich coatings have been used because their environment friendliness and no volatile organic compound contents. These coatings initially have a porous nature, so electrolyte permeates through the coating and reaches to the steel/coating interface. The zinc particles scarify themselves to provide cathodic protection of steel for a relatively short service time. As the exposure time increases, zinc corrosion products are formed and the nature of coating gradually convert to barrier. Subsequently, reduction in cathodic protection and losing electrical contact between zinc particles themselves or zinc particles and the steel substrate is due to accumulation of zinc corrosion products that have poor electrical conductivity.[4–7]

In zinc-rich coatings, the pigment volume concentration (PVC) of the Zn pigment in the coating should be more than the critical PVC (CPVC) to give electrical conduction between the zinc particles and between the zinc particles and the steel substrate to protect the underlying steel substrate.[7–10] If the ratio of PVC to CPVC be greater than one, there is no sufficient vehicle to wet the zinc particles and substrate so cause poor mechanical properties of the coating such as adhesion, cohesion, flexibility, abrasion resistance, and so forth. Also, uniform dispersion of the zinc particles in these high PVC paints is hard.[5,11,12]

Conventionally, alkali silicate salts and nano sized colloidal silica which can additionally contain a dissolve or dispersed organic resin or latex has been used as modifier materials for providing an aqueous inorganic coating. In this respect, a number of patent applications thereon have been filed.[13–16] To improve the corrosion resistance of the Zn-rich coatings, several investigations have been performed such as partial replacement of zinc particles by micaceous iron oxide or lamellar Al particles.[6,17,18] Also addition of nanoparticles like nanozinc/nanoclay[19,20] as well as binder formulation modification[17,21] has been investigated.

Modification of inorganic zinc coatings with small amounts of organic resins decreases the surface tension of the vehicle and increases the wettability of the vehicle. It has been reported that this type of alkali silicate binder modification improves the dispersion of the zinc pigments in the paint, cohesion of the film, adhesion to the substrate, and corrosion resistance of the coating.[17]

The aim of this work was to study the effect of modification of waterborne inorganic potassium silicate binder by adding of small amounts of organic acrylic based resins. The modified binder was used as binder for zinc-rich coating and corrosion resistance properties of these coatings were studied. The protective mechanisms of these coatings were examined by electrochemical impedance spectroscopy (EIS), open-circuit potential changes with the exposure time when immersed in artificial seawater, salt spray test, and scanning electron microscopy (SEM).

Table I. Typical Properties of Used Acrylic and Acrylic/Styrene Resins

Resin	Appearance	Type	Emulsifying system	Solids (%)	PH	T_g (°C)	Viscosity (cP)	MFFT (°C)
Acrylic	Milky white Liquid	Self-crosslink	Nonionic	45 ± 1	2-3	−14	1000	<0
Acrylic styrene	Milky Liquid	Self-crosslink	Anionic	47 ± 1	6-8	−2	3000	0

EXPERIMENTAL

Materials and Formulations

Commercial aqueous solutions of potassium silicate of 3.29 : 1 silica/alkali molar ratio were supplied by Iran silicate industries. For increasing the molar ratio of silica/alkali from 3.29 : 1 to 5.1 : 1, a 30% (w/w) colloidal acidic solution of nanosilica with particle size of about 10–20 nm (produced by Sharif Nano Pigment Company) was used. This binder was denoted as A5 which was obtained by adding gradually and mixing of nanosilica solution in potassium silicate solution slowly. The potassium silicate resin was modified by adding and mixing different amounts of commercial acrylic/styrene copolymer and acrylic emulsion which were supplied from Simab Resin Company (Tehran, Iran). Typical properties of used acrylic and acrylic/styrene resins are shown in Table I.

The modified binder solution was denoted as B1, B2, B3 and C1, C2, C3 which contained 5, 10, and 20% acrylic/styrene copolymer and acrylic emulsion, respectively. Compositions of formulated coatings are shown in Table II. In the composition of zinc-rich coatings, zinc dust with average particle diameters 4 μm (fine) was supplied from Pars Zinc Dust (Tehran, Iran). This powder was added to the vehicles to prepare unmodified and modified zinc-rich paint. Zinc dust content was at the level of 90% by weight to ensure efficient electrical conduction between zinc particles and steel substrate and also achieve good protection.

Application of the Coatings

The used metallic substrate was SAE 1010 steel with dimensions of 15 × 7 × 0.2 cm^3. Before applying the coating, the metal surface was sandblasted according to SA 2-1/2 (SIS Standard 05 59 00/1967). Coating was immediately applied over blasted steel panels by air spray equipment. Based on our observations, the initial curing time for modified samples with acrylic emulsion and acrylic/styrene copolymer was about 20 min (B and C series), whereas it was about 45 min for unmodified sample (A5). Two series of samples were prepared. The thickness of the obtained zinc-rich coatings was 50 ± 5 μm for series 1 and 70 ± 5 for series 2 plates. Series 1 plates were used for EIS tests and series 2 plates were used for salt spray tests. Before beginning the tests, the coated plates were placed in laboratory atmosphere for 7 days to ensure complete curing of binders.

Laboratory Tests

The EIS measurement was performed in a 3.5% NaCl solution at room temperature, using Autolab PGSTAT 302N potentiostat/galvanostat (Autolab, Italy). Also, corrosion potential (E_{corr}) measurements were performed for confirmation of cathodic protection period. Two clear polyvinyl chloride cylindrical tubes were fixed on each coated steel plate (to check repeatability). The exposed surface area of working electrode was 2 cm^2. FRA2 (frequency response analyzer) software (Eco Chemie B.V., The Netherlands) was used to perform EIS measurements. All the measurements were performed at open circuit potential at sinusoidal voltage amplitude equal to 10 mV over a frequency range of 10 MHz to 100 kHz at different immersion times. Electrochemical measurements were performed in a three electrode cell. The reference electrode was a saturated Ag/AgCl electrode and platinum rod was used as counter electrode.

For evaluating the corrosion protection performance of the coatings, the accelerated corrosion test in a salt spray chamber (B.AZMA CTS-114D, Iran) was conducted according to ASTM B117-03. The samples were exposed to the NaCl solution fog for about 1500 h and were investigated for rusting on the areas with cutting, without cutting and blistering according to ASTM D1654-08, ASTM D610-01, and ASTM D714-02, respectively.

The scanning electron microscope (SEM) studies were performed using a SEM model VEGA3 XM (TESCAN, Czech Republic). A scanning electron micrograph was taken of the panels coated with the zinc-rich paints before and after salt spray test and the surface configuration of these coatings was studied at 200× magnification.

RESULTS AND DISCUSSION

Electrochemical Impedance Spectroscopy

Nyquist plots of the EIS spectra for different coatings obtained at various immersion times in 3.5 wt % NaCl solutions are presented in Figures 1–7.

The Nyquist plots for all samples show one capacitive loop for short immersion times and the loop become smaller with increasing immersion time. Figures 1, 4, and 5 correspond with the model shown in Figure 8(a). After 18 and 13 days of

Table II. Specification of Formulated Coatings

Coating code	Zinc dust content (%)	Binder content (%)	Used modifier organic resin	Organic resin/total resin (%)
A5	90	10	-	-
B1	90	10	Acrylic/styrene	5%
B2	90	10	Acrylic/styrene	10%
B3	90	10	Acrylic/styrene	20%
C1	90	10	Acrylic	5%
C2	90	10	Acrylic	10%
C3	90	10	Acrylic	20%

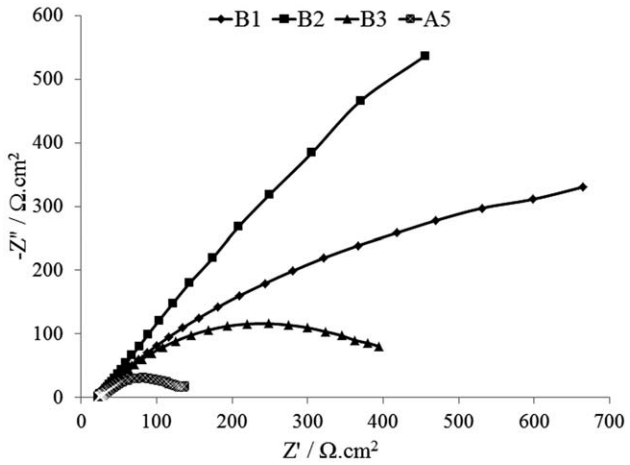

Figure 1. Nyquist plots of the EIS spectra for B series after 1 day immersion in 3.5 wt % NaCl solution.

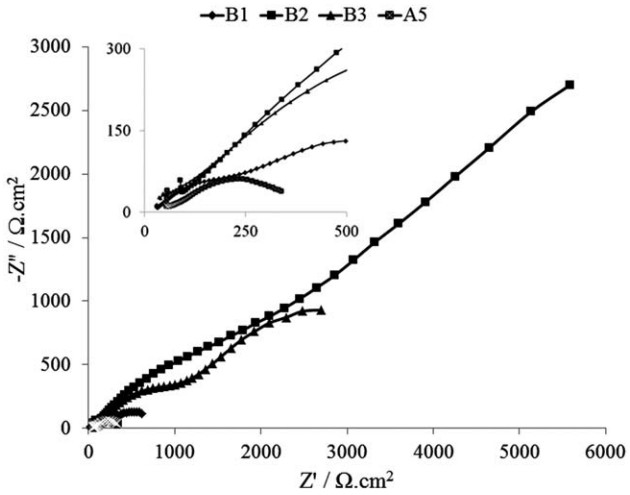

Figure 2. Nyquist plots of the EIS spectra for B series after 18 days immersion in 3.5 wt % NaCl solution.

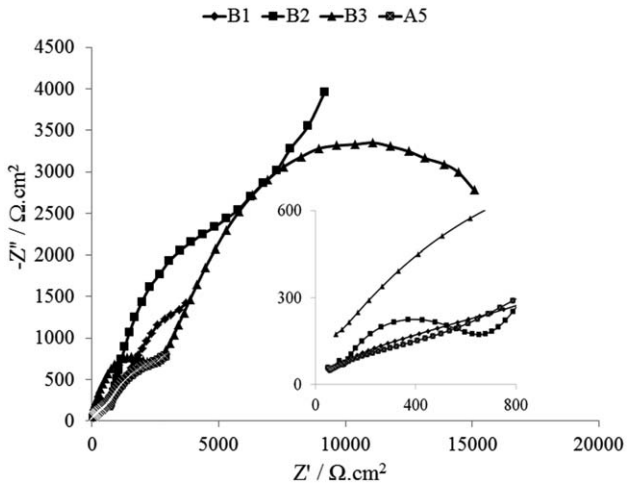

Figure 3. Nyquist plots of the EIS spectra for B series after 94 days immersion in 3.5 wt % NaCl solution.

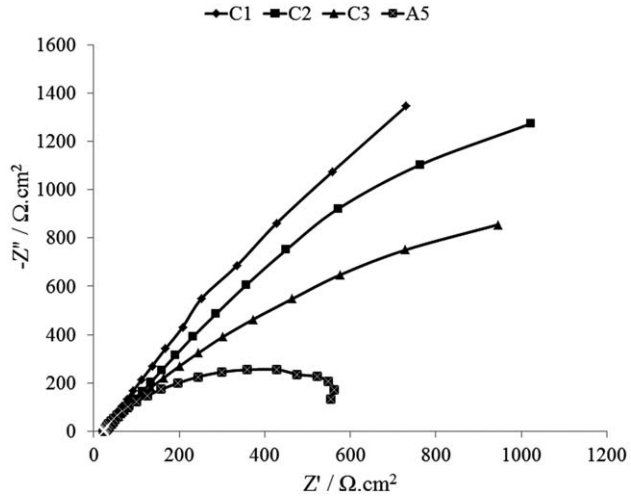

Figure 4. Nyquist plots of the EIS spectra for C series after 1 day immersion in 3.5 wt % NaCl solution.

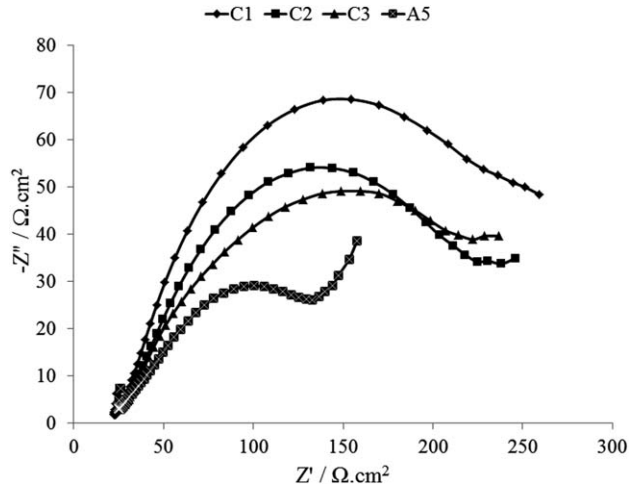

Figure 5. Nyquist plots of the EIS spectra for C series after 5 days immersion in 3.5 wt % NaCl solution.

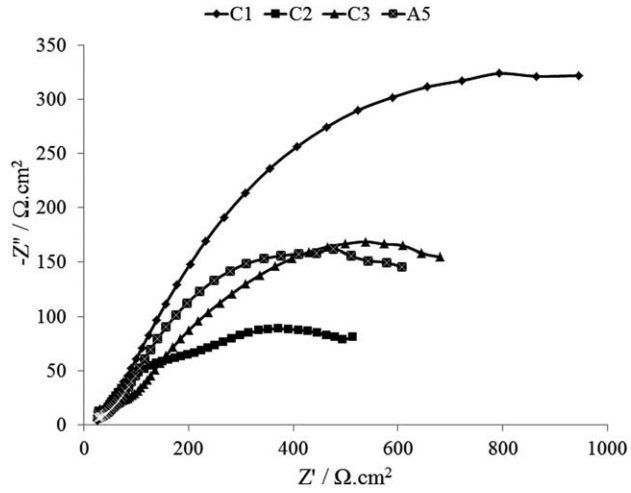

Figure 6. Nyquist plots of the EIS spectra for C series after 13 days immersion in 3.5 wt % NaCl solution.

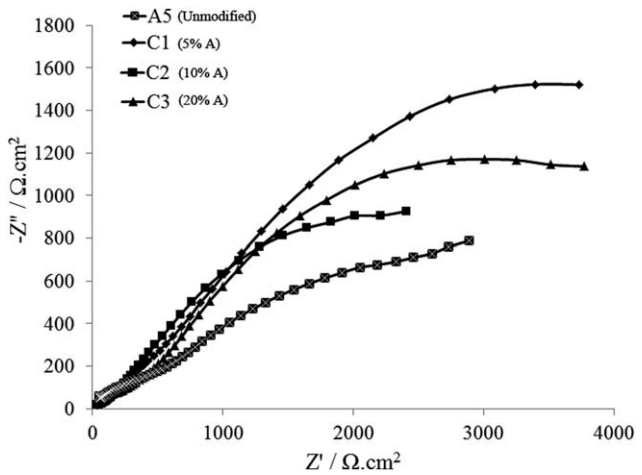

Figure 7. Nyquist plots of the EIS spectra for C series after 94 days immersion in 3.5 wt % NaCl solution.

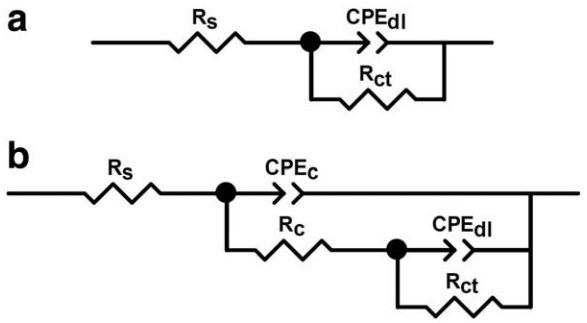

Figure 8. Equivalent circuits used for numerical fitting of the impedance plots obtained for the different immersion times (a) short immersion times (b) long immersion times.

immersion time for B and C series, respectively, the Nyquist plots show two semicircles corresponding to two capacitive time constants; Figures 2, 3, 6 and 7 that correspond to the model shown in Figure 8(b). In Figure 8, R_s represents the solution resistance; the constant phase element (CPE_c) is corresponded to the double layer capacity of the solution/coating interface responded at high frequency. CPE was used instead of the "ideal" capacitance considering heterogeneous, surface roughness, and porous nature of the zinc-rich coatings. R_c corresponds to the charge transfer resistance processes taking place within the pores of coating, R_{ct} and CPE_{dl} correspond to the resistance and the capacitance of substrate/coating interface in the range of low frequencies. The first loop in the high frequency range is related to the coating properties and the second loop at lower frequencies is related to the corrosion process (zinc dissolution process), as shown in Figures 2, 3, 6, and 7. The impedance reduction for first few days is due to zinc particles activation, and then it increases because of reduction the active surface area due to zinc consumption and zinc corrosion products formation in the pores of the coatings. Spectra depression is due to the porous nature of the coatings.[7,22] The EIS data were fitted using Zview and Zsim softwares.

Table III shows the EIS extracted parameters for B series (modified with acrylic/styrene). The results indicate that the charge transfer resistance of B2 (containing 10% of acrylic styrene) is higher than the others during 18 days of immersion time and it showed better corrosion resistance than the others. As mentioned in Table III, from day 18 to 94 the charge transfer resistance of B3 (containing 20% acrylic styrene) is a little more than B2 and it seems that the corrosion product of B3 is more stable than B2. Table III shows that all the B series samples had extremely higher charge transfer resistance than A5 (containing no organic resin) and showed a better corrosion

Table III. Parameters Values Obtained from Fittings of EIS Spectra of B Series

Immersion time (days)	Coatings	R_s	R_{ct}	CPE_{dl}-Q	CPE_{dl}-n	R_c	CPE_c-C	CPE_c-n
1	B1	23.66	915.4	0.0027204	0.59413			
	B2	22.98	11,431	0.0051456	0.62367			
	B3	23.48	448.9	0.0021085	0.60851			
	A5	24.79	123.1	0.003052	0.5692			
18	B1	20.89	384.6	0.0005685	0.398	396.9	0.003743	0.6558
	B2	53.07	4667	0.0001296	0.407	1.033E4	0.0005318	0.6945
	B3	66.55	1516	0.0001382	0.4826	2867	0.001251	0.6919
	A5	43.38	68.19	4.712E-5	0.4041	340.4	0.001763	0.408
57	B1	42.18	157.3	2.056E-6	0.7717	3821	0.000207	0.3292
	B2	31.71	252.7	8.008E-7	0.7542	1.204E4	9.505E-5	0.5314
	B3	38.71	614.9	1.614E-6	0.645	1.346E4	0.0001156	0.4994
	A5	44.68	300.5	0.000116	0.5229	4515	0.0004711	0.609
94	B1	54.31	925.8	6.631E-5	0.421	8806	0.000464	0.4423
	B2	84.42	549.8	7.313E-7	0.8048	1.093E4	0.0001025	0.5831
	B3	65.92	2420	8.369E-7	0.6644	1.635E4	5.865E-5	0.4999
	A5	51.35	373.4	1.86E-5	0.5046	5141	0.0003865	0.3477

Table IV. Parameters Values Obtained from Fittings of EIS Spectra of C Series

Immersion time (days)	Coatings	R_s	R_{ct}	CPE_{dl}-Q	CPE_{dl}-n	R_c	CPE_c-C	CPE_c-n
1	C1	22.54	16,967	0.0030781	0.75377			
	C2	26.58	15,531	0.0025245	0.68899			
	C3	23.78	3850	0.0027572	0.67711			
	A5	23.01	690	0.0026259	0.75986			
5	C1	23.29	277.1	0.0022659	0.57572			
	C2	25.01	246.9	0.0018852	0.51166			
	C3	23.74	270.2	0.0026894	0.43858			
	A5	22.07	189.7	0.0038246	0.35345			
13	C1	21.8	65.32	0.0008837	0.4563	1516	0.0005316	0.6104
	C2	25.92	104.5	0.0015	0.2326	870.6	1.538E-5	0.7627
	C3	23.41	200.6	0.001058	0.2784	1042	0.0005723	0.5885
	A5	17.54	64.71	0.0008737	0.367	817.3	0.0007827	0.5876
57	C1	15.5	2268	0.0004089	0.3568	7562	8.847E-5	0.8256
	C2	20.54	136.3	0.0002055	0.4293	4208	0.0004781	0.5012
	C3	16.58	229.2	1.925E-5	0.5148	2671	0.0003334	0.4518
	A5	44.68	300.5	0.000116	0.5229	4515	0.0004711	0.609
94	C1	14.78	1416	0.0003463	0.3625	1.17E4	0.0001112	0.6771
	C2	12.64	160.5	0.0001797	0.4002	5247	0.0004496	0.4947
	C3	14.84	329.8	3.29E-5	0.4709	6311	0.0003233	0.475
	A5	17.26	373.4	1.86E-5	0.5046	5141	0.0003865	0.3477

protection than it. This is related to the second mechanism of protection, formation, and accumulation of corrosion products (barrier protection).

The EIS results from C series (modified with acrylic) indicated that the charge transfer resistance of C1 with 5% of acrylic resin is higher than the others for all immersion times and it showed better corrosion resistance than the others (Table IV). This means adding 5% of acrylic resin to inorganic resin improves corrosion prevention, but adding more than 5% did not improves corrosion prevention effectively. The samples in this group especially C1 had better corrosion protection than A5 because of their better barrier protection.

Table V shows that, in first day of immersion, the charge transfer resistances of C series was more than B series, this can be related to easier electrolyte penetrating through the porous coating of C series and wetting steel substrate, but then charge transfer resistances of B series became more, due to better barrier protection of B series. C1 with 5% of acrylic resin has better protection than B1 with 5% acrylic styrene but C2 and C3 with 10, 20% acrylic has smaller charge transfer resistances than B2 and B3 containing 10, 20% acrylic/styrene.

Corrosion Potential (E_{corr}) Measurements

To investigate the cathodic protection duration and electrochemical activity of the modified coatings, E_{corr} measurements were performed. Figure 9 shows variation in corrosion potentials during immersion time for samples with different formulations exposed to 3.5% NaCl solution. Changes of E_{corr} values depend on the ratio of zinc to steel (active areas).[10] According to the commonly accepted criterion to provide cathodic protection, E_{corr} value should remain lower than −0.735 V (Ag/AgCl) equivalent to −0.780 V (SCE).[23]

Table V. Comparison of R_{ct} and R_c Between B and C Series

Immersion time (days)	Resistance values Ω	Coatings code					
		B1	C1	B2	C2	B3	C3
1	R_{ct}	915.4	16,967	11,431	15,531	448.9	3850
	R_c	–	–	–	–	–	–
57	R_{ct}	157.3	2268	252.7	136.3	614.9	229.2
	R_c	3821	7562	1.204E4	4208	1.346E4	2671
94	R_{ct}	925.8	1416	549.8	160.5	2420	329.8
	R_c	8806	1.17E4	1.093E4	5247	1.635E4	6311

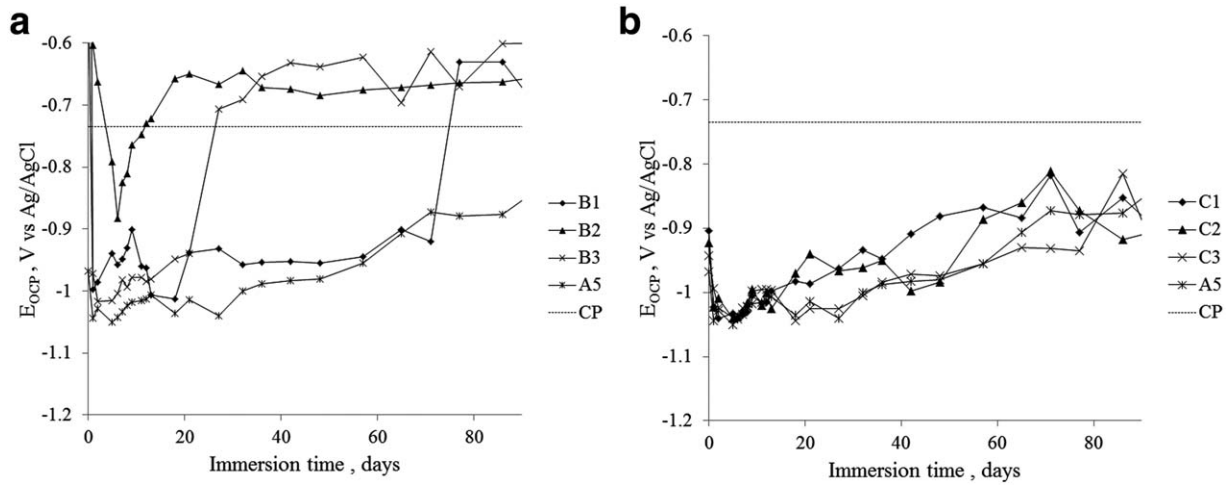

Figure 9. Variations in corrosion potential with time for (a) B series (b) C series.

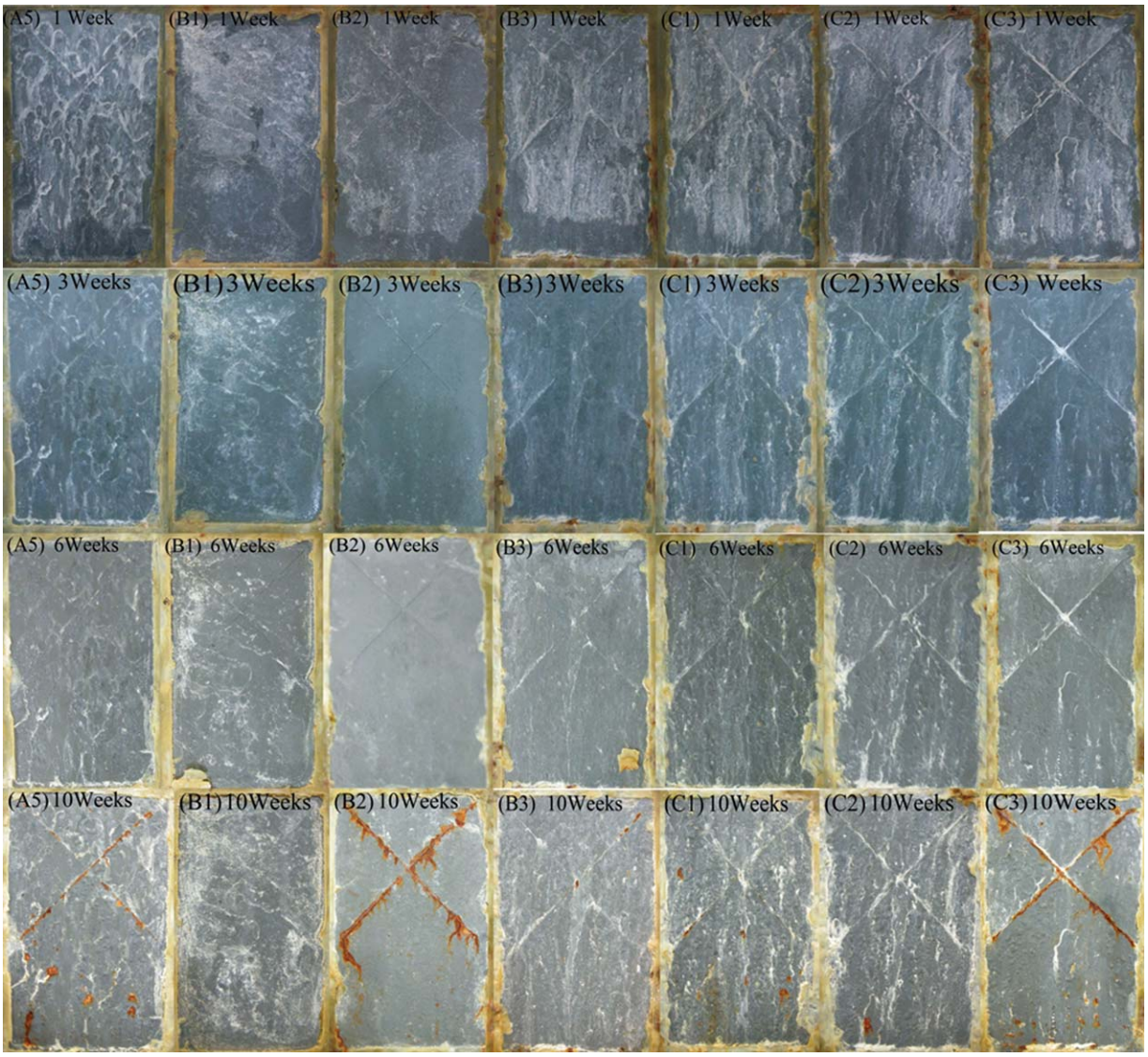

Figure 10. The photographs of the samples during 1500 h exposition in the salt spray (fog) chamber. [Color figure can be viewed in the online issue, which is available at wileyonlinelibrary.com.]

Table VI. Anticorrosive Performance Evaluation of Salt-Spray Chamber Tested Paint Coatings

Coatings code	Blisters in paint area (ψ1), ASTM D714	Blisters near section (ψ2), ASTM D714	Primer corrosion in section (ψ3), ASTM D1645	Primer corrosion in area (ψ4), ASTM D610	Anticorrosion Efficiency α
A5	2MD	2M	8 (1 mm)	5-G (3%)	38.75
B1	6M	6MD	10 (0)	9-S (0.03)	61.25
B2	6MD	6M	6 (3)	8-G (0.1)	46.25
B3	4MD	4M	9 (0.5)	9-G (0.03)	50.63
C1	4D	4MD	9 (0.5)	7-G (0.3)	48.75
C2	6MD	6M	10 (0)	7-S (0.3)	56.75
C3	2M	2F	7 (2)	6-G (1)	50.63

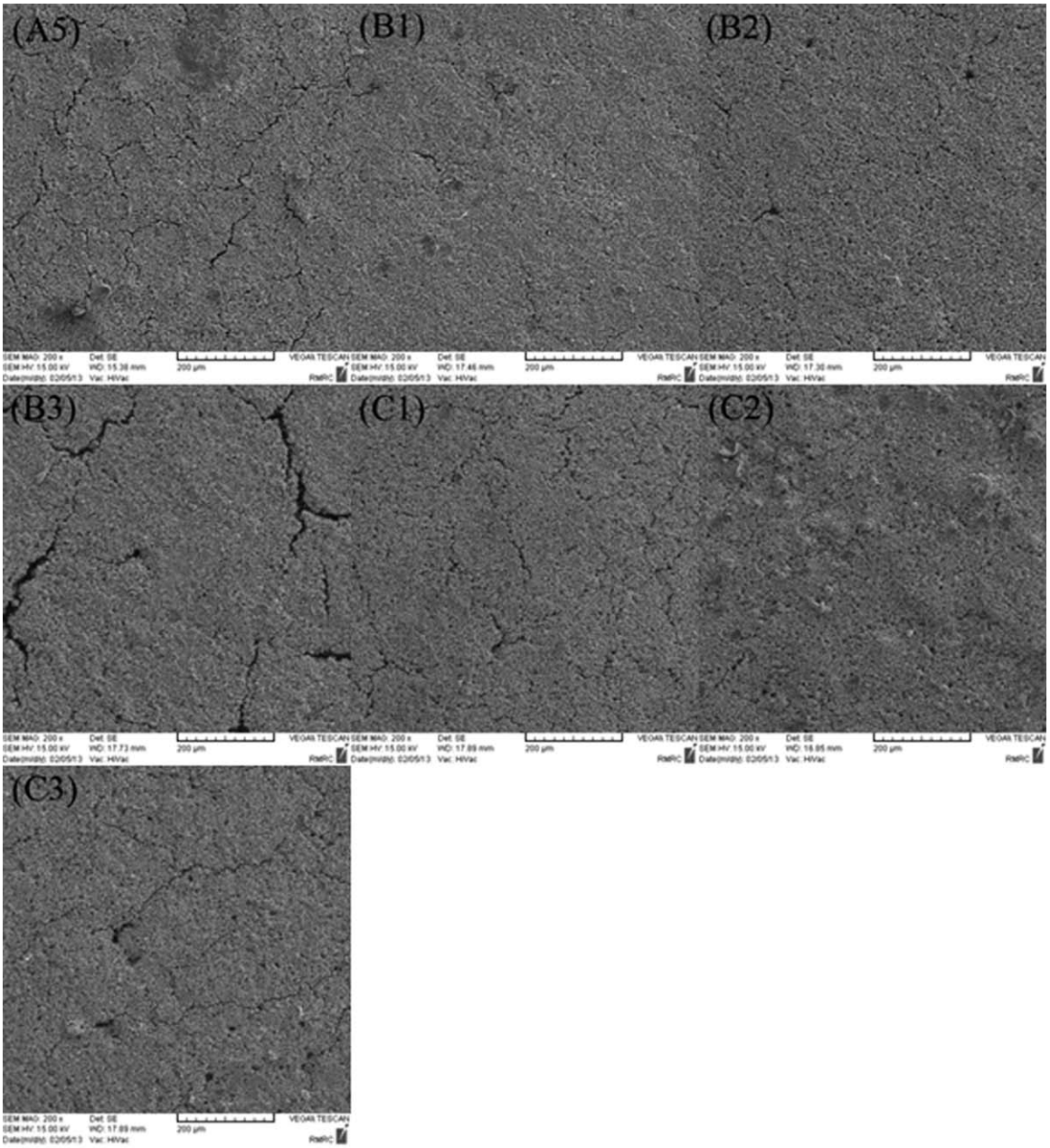

Figure 11. SEM images for the samples before exposure to salt spray.

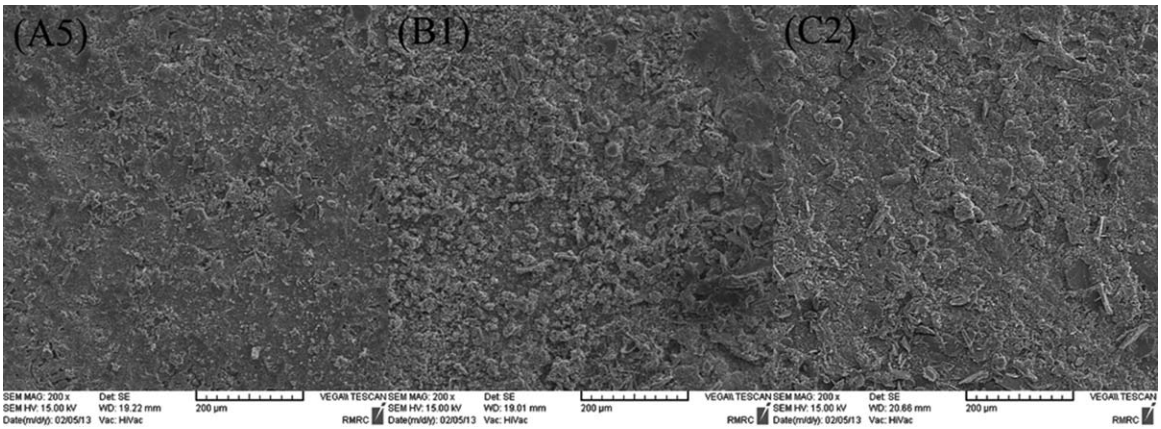

Figure 12. SEM images for the samples after exposure to salt spray.

As shown in Figure 9, in both series at first, the corrosion potential shifted cathodically to negative values as a result of increasing Zn/Fe area ratio due to activating the zinc particles by reaction with the electrolyte. Then, the corrosion potential increased reaching the potential over which cathodic protection is no longer efficient as a result of Zn/Fe area ratio decrease caused by zinc corrosion and isolation of the zinc particles by the zinc corrosion products.

In the B series, B1 with 5% acrylic/styrene has longer cathodic protection duration than B2 and B3. B1 has 77 days cathodic protection duration, but B2 and B3 have very short cathodic protection duration, 12 and 27 days, respectively. The unmodified sample A5 did not lose its cathodic protection during immersion time. This can be explained by reduction in zinc pigments connections and stabilization of corrosion products as a result of high wettability of modified resin with acrylic/styrene. Figure 9(a,b) shows that, in C series, none of the samples lost their cathodic protection during immersion time. It seems that C3 with 20% acrylic resin has a better cathodic protection than the others.

Salt-Spray Chamber Test

The photographs of the samples during 1500 h exposure in the salt spray (fog) chamber are presented in Figure 10. After 1000 h (6 weeks) of exposure in salty fog cabinet, some blistering but no rusting has been observed on the coatings. Using ASTM D610-01, the amount and distribution of visible surface rust were quantified. The degree of rusting corresponding to the areas without cutting was determined using rust grade of 0–10 where 0 indicates that greater than 50% of surface rusted and 10 indicates that less than or equal to 0.01% of surface rusted, followed by the type of rust distribution identified by *S* for spot, *G* for general, *P* for pinpoint or *H* for Hybrid. The results are displayed in Table VI; according to this standard, all samples showed better corrosion resistance in unscribed areas than the unmodified sample (A5). Moreover, results of Table VI allow concluding that series B almost showed better anticorrosive function in unscribed areas than series C which is in agreement with EIS results. Rust creepage at scribed areas can be determined using ASTM D1654-08 by measuring overall width of the corrosion zone and width of the original scribe. Creep values are reported in millimeters and rating numbers. All samples except B2 and C3 showed better protective performance against rust creepage than unmodified sample. No signs of rust creepage at scribes of B1 and C2 were observed after 1500 h exposition exposure and they had the best performance. Using ASTM D714-02, we identified the size and density (frequency) of the blisters on the coatings. The size of the blisters was identified by numbers from 10 to 0, in which No. 10 represents no blistering. Nos. 8 and 2 represent the smallest and largest size blister, respectively. The frequency of blister occurrence was identified by some letters which come after the number of blister size. The greatest frequency of blister occurrence is showed with letter D (dense), whereas less dense blister is marked as MD (medium dense), M (medium), and F (few).[24] The degree of blister on the coating increases according to the following order B1 < C3 < C2 < B2 < B3 < A5 < C1.

We also did this for near section areas of the coatings to obtain anticorrosion efficiencies.[20] The degree of blister in near section areas of coatings increases according to the following order C3 < C2 < B2 < B3 < A5 < B1 < C1.

On overall, the samples take the following order of salt spray resistance B1 > C2 > B3 > C3 > C1 > B2 > A5.

The enhancement of corrosion resistance of the modified binder coatings may be due to high wettability of modified binders which help to enhance coating adhesion to the substrate and increase the barrier properties of the coatings.

SEM Observation

To give more insight on differentiation of modified and unmodified vehicles (binders), SEM was conducted. Figure 11 illustrates the SEM images for the samples before exposure to salt spray. As shown in these figures, it is seen that the zinc particles are closely packed on the surface. As one can be seen from Figure 11, few cracks can be found in the original coatings surfaces. B1 and C2 have fewer cracks and holes which confirm the salt spray results. These cracks were even more obvious in the unmodified coating and amount of them on the coating were increased, so suppressed corrosion resistance. This is due to defective wetting characteristics of the binder and not good dispersion of Zn pigments. After salt spray exposure, cracks

were filled with zinc corrosion products and protect the steel substrate by barrier mechanism. Figure 12 illustrates SEM images for B1 and C2 which had the best salt spray test results after exposure to 1500 h salt spray. It seems that B1 and C2 sealed the pores and cracks better than A5 (sample), thus have better barrier protection and there is still some unreacted zinc.

CONCLUSIONS

The influence of the modification of eco-friendly waterborne alkali silicate zinc-rich coating by adding small amounts (5, 10, and 20 wt %) of acrylic and acrylic/styrene copolymer was studied. Motivation for doing this work was removing the poor wettability of inorganic silicate based zinc-rich coatings. However, the main expectations were increasing wettability of the vehicle of the zinc pigments, cohesion and adhesion of the film to steel substrates.

1. Presence of water-based acrylic derivatives into the potassium silicate zinc-rich coating did not lead to the improvement of cathodic protection duration.
2. EIS and salt spray results showed that, in alkali silicate zinc-rich coatings, the modification of silicate binder with acrylic derivatives led to better corrosion resistance due to the better sealing action of zinc corrosion products and also enhancing coating adhesion to the substrate.
3. SEM observations showed that the modified coatings, with acrylic binders, had better Zn pigments dispersion in vehicle and fewer cracks.
4. Adding of 5% acrylic/styrene copolymer and 10% acrylic resin improved salt spray test results of formulated zinc-rich coatings.

REFERENCES

1. Chua, H. H.; Johnson, B. V.; Ross, T. K. *Corros. Sci.* **1978**, *18*, 505.
2. Gergely, A.; Pfeifer, É.; Bertóti, I.; Török, T.; Kálmán, E. *Corros. Sci.* **2011**, *53*, 3486.
3. Hammouda, N.; Chadli, H.; Guillemot, G.; Belmokre, K. *Adv. Chem. Eng. Sci.* **2011**, *1*, 51.
4. Morizane, T.; Yamada, Y.; Takagishi, J.; Matsuno, H.; Ohshiba, M. US Patent 0,030,584, 2011.
5. Canosa, G.; Alfieri, P. V.; Giudice, C. A. *Prog. Org. Coat.* **2012**, *73*, 178.
6. Kakaei, M. N.; Danaee, I.; Zaarei, D. Corros. Eng., *Sci. Technol.* **2012**, *48*, 194.
7. Gervasi, C. A.; DI Sarli, A. R.; Cavalcanti, E.; Ferraz, O.; Bucharsky, E. C.; Real, S. G.; Vilche, J. R. *Corros. Sci.* **1994**, *36*, 1963.
8. Pedram, R.; Ross, T. K. *Corros. Sci.* **1978**, *18*, 519.
9. Shreepathia, S.; Bajajb, P.; Mallika, B. P. *Electrochim. Acta* **2010**, *55*, 5129.
10. Abreu, C. M.; Izquierw, M.; Keddam, M.; Novo, X. R. *Electrochim. Acta* **1996**, *41*, 2405.
11. Knudsen, O. Ø.; Steinsmo, U.; Bjordal, M. *Prog. Org. Coat.* **2005**, *54*, 224.
12. O'Donoghue, M.; Garrett, R.; Datta, V. J.; Osborne, S.; Roberts, P. Paint and Coatings Expo, Las Vegas, Nevada, USA, **2005**, 23–26.
13. Kemp, W. E. US Patent 3,231,535, 1966.
14. Davies, G. H.; Jackson, P. A. US Patent 8,128,996, 2012.
15. Beers, R. W.; Lakritz, J. US Patent 3,884,863, 1975.
16. Neel, J.; Bonnel, B. US Patent 3,450,661, 1969.
17. Zhang, L.; Ma, A.; Jiang, J.; Song, D.; Chen, J.; Yang, D. *Prog. Nat. Sci.* **2012**, *22*, 326.
18. Arman, S. Y.; Ramezanzadeh, B.; Farghadani, S.; Mehdipour, M.; Rajabi, A. *Corros. Sci.* **2013**, *77*, 118.
19. Arianpouya, N.; Shishesaz, M.; Arianpouya, M.; Nematollahi, M. *Surf. Coat. Technol.* **2013**, *216*, 199.
20. Schaefer, K.; Miszczyk, A. *Corros. Sci.* **2013**, *66*, 380.
21. Hoshyargara, F.; Sherafati, S. A.; Hashemi, M. M. *Prog. Org. Coat.* **2009**, *65*, 410.
22. Selvaraj, M.; Guruviah, S. *Surf. Coat. Int.* **1997**, *80*, 12.
23. Feliu S. Jr., Morcillo, M.; Feliu, S. *Corrosion (Houston, TX, U. S.)* **2001**, 57.
24. Kalendová, A.; Kalenda, P.; Veselý, D. *Prog. Org. Coat.* **2006**, *57*, 1.